Wear, *173* (1994) 151–165

Effects of lubricant compressibility on the film thickness in EHL line and circular contacts

C.H. Venner and J. Bos

Faculty of Mechanical Engineering, University of Twente, P.O. Box 217, 7500 AE Enschede (Netherlands)

(Received September 8, 1993; accepted December 16, 1993)

Abstract

As a first step towards generalized (non-closed-form coefficients in Reynolds' equation) lubricant behaviour, this paper describes the incorporation of the Jacobson and Vinet density pressure equation in a multilevel solver for the pressure and the film thickness in an EHL contact. However, the use of this model is also of interest on its own account, as compression experiments (Jacobson and Vinet, Ramesh) have indicated limitations to the applicability of the widely used Dowson and Higginson equation. In this paper, results of the isothermal steady-state line and circular contact are presented and compared with results obtained assuming an incompressible lubricant and with results employing lubricant compressibility according to the Dowson and Higginson equation. The observed phenomena are traced back to Reynolds' equation, and it is shown that the reduction of the central film thickness due to compressibility can be predicted easily, regardless of the type of density pressure equation used. In addition it is shown that, using the Jacobson and Vinet equation, the minimum film thickness in a line contact, beyond a certain load, may occur in the centre of the contact, instead of at the exit. This phenomenon is analysed theoretically, and it is shown to be very unlikely to occur in the circular-contact problem.

1. Introduction

Over the last decade, numerical simulation of EHL contacts has been the subject of quite intensive research. Efficiency and stability of numerical algorithms have been greatly improved, and, also because of the development of faster hardware over the years, increasingly complex simulations can be performed nowadays. No doubt these simulations have contributed to an increased understanding of the mechanisms influencing the operation of EHL contacts on a global as well as on a local scale (micro-EHL). Nevertheless, even for fully flooded contacts, there is still a significant gap to be bridged between what is taken into account in numerical simulations and what may actually happen in "real contacts". Consequently, further developments are needed. Directions to be considered are many, *e.g.* detailed analysis of the transient effects of surface features in circular and elliptical contacts, validation of the physical–mathematical models by directly comparing their predictions with experimental results; questions remain to be answered about lubricant behaviour, and its effect on film thickness, pressure, and friction under different conditions. The present paper attempts to contribute to the latter subject and focuses on the compressibility of the lubricant.

So far results presented in literature, *e.g.* Lubrecht [1], Hamrock *et al.* [2], Kweh *et al.* [3], show that, for most practical load conditions, compressibility has a very minor effect on the minimum film thickness. However, the film thickness in the centre of the contact is quite significantly reduced. For example, Kweh *et al.* [3] demonstrate that in a circular contact the reduction in central film thickness due to compressibility can be correlated with the increase in density at the local pressure in the centre of the contact.

In these studies and, to the authors' knowledge, in most studies accounting for compressibility, the density pressure equation presented by Dowson and Higginson [4] is used. Characteristic of this equation is that the increase of the density with pressure rapidly levels off with increasing pressure. Moreover, the density reaches a limit, and for sufficiently high pressures the lubricant in effect behaves as incompressible again. In recent years, experimental evidence (Jacobson and Vinet [5], Ramesh [6]) has indicated that this behaviour may be questionable, particularly for synthetic lubricants. As a result, indiscriminately applying the Dowson and Higginson relation may result in an underestimation of the film thinning in the centre of the contact.

*Available from Central Library, University of Twente, P.O. Box 217, 7500 AE Enschede, Netherlands.

SSDI 0043-1648(93)06412-W

In this paper, results are presented for both the line- and circular-contact problems obtained using the alternative density–pressure model proposed by Jacobson and Vinet [5]. These results are compared with results obtained using the equation of Dowson and Higginson and results for an incompressible lubricant. The observed phenomena are traced back to Reynolds' equation and it is shown that, for both line and point contacts, the reduction of the central film thickness due to compressibility can be predicted accurately with a simple formula which confirms the correlation between density at central pressure and central film thickness reported by Kweh *et al.* [3].

These compressibility effects were not the only reason for this study. The density–pressure equation proposed by Jacobson and Vinet is formulated inversely, *i.e.* it gives pressure as a function of density. At first sight this seems rather inconvenient, as in Reynolds' equation the density itself appears in the coefficients. From a numerical solution point of view the same situation arises if non-newtonian lubricant behaviour and thermal effects are to be accounted for. No matter how important these effects may be, with respect to the solution of the pressure and film thickness in the contact, their appearance in Reynolds' equation is via the *coefficients* in the pressure flow term and in the form of the equivalent of a *density* in the wedge term; see, for example, Yang and Wen [7]. In the simple newtonian isothermal case when assuming an incompressible lubricant and a direct density–pressure equation (such as the Dowson and Higginson equation) these coefficients and this density are given in closed form equations in terms of the pressure, the viscosity and the film thickness. However, in the non-newtonian thermal case and also when the Jacobson–Vinet density–pressure equation is used, they are to be solved (iteratively) from equations.

In this paper it is explained how the necessary iterative process related to non-closed-form coefficients in Reynolds' equation can be incorporated in a solver for the pressure and the film thickness at minimum computational expense. Hence, the incorporation of the Jacobson and Vinet density–pressure equation also serves as a first step towards the efficient incorporation of complex lubricant behaviour in EHL simulations, *i.e.* an example from which the essentials are to be understood.

2. Equations

2.1. Line contact

Using the hertzian parameters (see Appendix: Nomenclature) to obtain dimensionless variables, the generalized Reynolds' equation (see Yang and Wen [7]) for the steady-state EHL line contact can be written as

$$\frac{\partial}{\partial X}\left(\epsilon\frac{\partial P}{\partial X}\right)-\frac{\partial(\bar{\rho}^{*}H)}{\partial X}=0 \tag{1}$$

with boundary conditions $P(X_a)=P(X_b)=0$ and the cavitation condition $P\geqslant 0$. Depending on the specific effects taken into account, ϵ may depend on pressure, temperature, slip, film thickness, etc., and $\bar{\rho}^{*}$ is an equivalent density. However, in the simple case of newtonian lubricant behaviour and an isothermal contact, $\bar{\rho}^{*}=\bar{\rho}$ and

$$\epsilon=\frac{\bar{\rho}H^{3}}{\bar{\eta}\lambda} \tag{2}$$

where

$$\lambda=\frac{6\eta_0 u_s R^{2}}{b^{3}p_h} \tag{3}$$

Throughout this work we will assume the dimensionless lubricant viscosity $\bar{\eta}$, to be given by the Roelands [8] equation with $\alpha=1.7\times10^{-8}$ and $z=0.69$. The dimensionless lubricant density $\bar{\rho}$ will be unity in the incompressible case. If the lubricant is assumed to behave compressibly, it is obtained either from the Dowson and Higginson equation (in dimensionless form):

$$\bar{\rho}=\frac{0.59\times10^{9}+1.34Pp_h}{0.59\times10^{9}+Pp_h} \tag{4}$$

or from the equation proposed by Jacobson and Vinet [5]; see Section 2.3.

Expressed in the same dimensionless variables, the film thickness equation reads

$$H=H_0+0.5X^{2}-\frac{1}{\pi}\int_{X_a}^{X_b}\ln|X-X'|P(X')\,\mathrm{d}X' \tag{5}$$

where H_0 is an integration constant determined by the force balance equation, which in its dimensionless form reads

$$\int_{X_a}^{X_b}P(X)\,\mathrm{d}X-\frac{\pi}{2}=0 \tag{6}$$

2.2. Circular contact

As for the line contact discussed above, the dimensionless generalized Reynolds' equation for a steady-state circular contact can be written as:

$$\frac{\partial}{\partial X}\left(\epsilon\frac{\partial P}{\partial X}\right)+\frac{\partial}{\partial Y}\left(\epsilon\frac{\partial P}{\partial Y}\right)-\frac{(\bar{\rho}^{*}H)}{\partial X}=0 \tag{7}$$

with the cavitation condition $P \geqslant 0$ and $P=0$ on the boundary of the domain. In the isothermal case for a newtonian lubricant, $\bar{\rho}^* = \bar{\rho}$ and ϵ is defined by:

$$\epsilon = \frac{\bar{\rho} H^3}{\bar{\eta}\lambda} \tag{8}$$

with

$$\lambda = \frac{6\eta_0 u_s R_x^2}{a^3 p_h} \tag{9}$$

As for the line contact, the dimensionless lubricant viscosity $\bar{\eta}$ is assumed to be given by the Roelands [8] equation. The dimensionless density is unity for an incompressible lubricant. For a compressible lubricant it will be obtained either from the Dowson and Higginson equation or from the Jacobson and Vinet equation.

The dimensionless film thickness equation reads

$$H(X, Y) = H_0 + \frac{X^2}{2} + \frac{Y^2}{2} + \frac{2}{\pi^2}\int_{-\infty}^{\infty}\int_{-\infty}^{\infty} \frac{P(X', Y')\, dX'\, dY'}{[(X-X')^2+(Y-Y')^2]^{1/2}} \tag{10}$$

Finally the dimensionless force balance equation reads

$$\int_{X_a}^{X_b}\int_{Y_a}^{Y_b} P(X, Y)\, dX\, dY - \frac{2\pi}{3} = 0 \tag{11}$$

2.3. *Density–pressure relation*

Jacobson and Vinet [5] propose the following equation to model the compressibility of the lubricant

$$p = 3B_0\bar{\rho}^{2/3}(1-\bar{\rho}^{-1/3}) \exp[\eta'(1-\bar{\rho}^{-1/3})] \tag{12}$$

where $\bar{\rho} = \rho/\rho_0$ is the dimensionless density. B_0 and η' are parameters with characteristic values for a mineral oil of $B_0 = 1.7\times10^9$ and $\eta' = 10.0$. These values will be used throughout the present work. For obtaining the density equation, eqn. (12) is slightly inconvenient, as it cannot easily be inverted analytically. However, for a given pressure, a numerical value for $\bar{\rho}$ can be obtained with reasonable ease using, for example, a Newton–Raphson iteration.

Figure 1 compares the dimensionless lubricant density $\bar{\rho}$ as a function of the pressure according to eqn. (12) (the dashed line), for B_0 and η' as given above, with the density obtained from the Dowson and Higginson equation (the solid line). Up to about 0.3 GPa both relations give almost the same density. Beyond this value the predictions differ increasingly. Where the Dowson–Higginson equation rapidly approaches an asymptotic compression of about 30%, eqn. (12) allows a much larger compression. A similar curve indicating larger compression at high pressures compared to the Dowson–Higginson equation was presented in Fig. 11 of Ramesh [6].

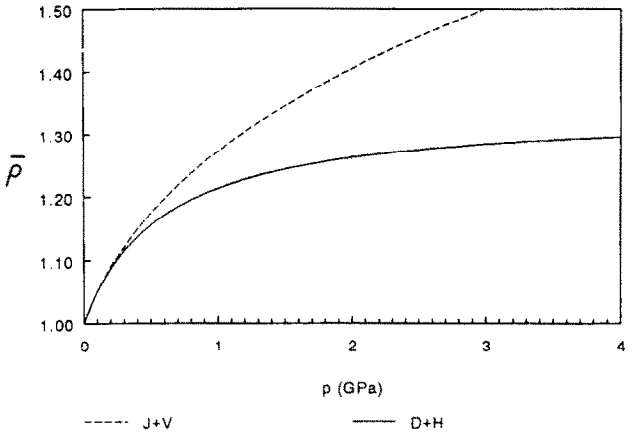

Fig. 1. Dimensionless lubricant density as a function of pressure according to the Jacobson and Vinet relation and the Dowson and Higginson equation.

According to Jacobson and Vinet [5], this larger compressibility can be expected to have a significant effect in the central region of the contact: "If the compressibility is high enough, the minimum film thickness will not appear at the outlet of the elastohydrodynamic contact, but in the centre of the contact".

3. Numerical approach

In recent years it has been amply demonstrated that multigrid techniques yield fast and efficient solvers for EHL problems. Following the introduction by Lubrecht [1,9,10], they have found increasing application in EHL, *e.g.* Osborn and Sadeghi [11], Kim and Sadeghi [12], Ai and Cheng [13], and Huang *et al.* [14]. A detailed explanation of these techniques and their application to the EHL line and point contact problem can be found in Venner [15] and Lubrecht [1] and references cited therein. In this section we start out from the discretizations and algorithms for the line and circular contacts described in Venner [15–18] and focus on the questions to be answered when changing the model, *e.g.* by adding equations to the system.

The cornerstone of an efficient multilevel solver for any integro-partial differential equation is a relaxation process that effectively smooths the error. In the case of a system of equations, this firstly applies to each individual equation and the variable assigned to it. At this stage, matters such as anisotropy in the equations (strong coupling in one of the directions) have to be recognized and dealt with. Secondly, for a system of equations it should be investigated how the relaxation of one equation for its variable affects the residuals of the other equations. This generally depends on the strength of the coupling between the equations. A

formal tool to investigate this coupling is an analysis of the determinant of the system of equations, see Brandt [19].

To illustrate this point of coupling: when developing a relaxation process for Reynolds' equation and the film thickness equation, it is convenient to have the relaxation deal with each equation consecutively, *e.g.* first compute the entire elastic deformation and film thickness and subsequently scan the grid to improve the pressure everywhere using the (discretized) Reynolds equation. For such a relaxation (when repeated) to converge and smooth well, it is essential that the changes applied to the pressure are such that their cumulative effect on the elastic deformation integrals remains small. At low loads, this is automatically the case and most standard relaxation processes will converge. However, with increasing load the coupling between Reynolds' equation and the film thickness equation (via the elastic deformation integrals) becomes stronger and distributive relaxation is needed. These matters are extensively explained in Venner [15].

From a fundamental point of view, the questions raised above need to be readdressed when adding an equation to the system. However, in the present case, the answers are easily found. Firstly, the matter of relaxation. Equation (12), made dimensionless, can be discretized as:

$$L_{\bar{\rho}}=p_{\mathrm{h}}P_{\mathbf{i}}-3B_0\bar{\rho}_{\mathbf{i}}^{2/3}(1-\bar{\rho}_{\mathbf{i}}^{-1/3})\exp[\eta'(1-\bar{\rho}_{\mathbf{i}}^{-1/3})]=0 \tag{13}$$

where $\mathbf{i}$ denotes the grid index. ($\mathbf{i}=i$ in one dimension; $\mathbf{i}=(i,j)$ in two dimensions, etc.) Let P_i stand for a given (dimensionless) pressure distribution on the grid and $\bar{\rho}_{\mathbf{i}}$ for an approximation to the associated (dimensionless) density distribution $\bar{\rho}_i$. A relaxation sweep over the density–pressure equation is then defined as: for all i, change $\bar{\rho}_i$ according to

$$\bar{\rho}_{\mathbf{i}} \longleftarrow \bar{\rho}_{\mathbf{i}}+r_{\mathbf{i}}\left(\frac{\mathrm{d}L_{\bar{\rho}}}{\mathrm{d}\bar{\rho}}\right)^{-1}\Bigg|_{\bar{\rho}_{\mathbf{i}}} \tag{14}$$

Note that this is simply applying a single Newton–Raphson change to each point. r_i is the residual of eqn. (13) defined as:

$$r_{\mathbf{i}}=3B_0\bar{\rho}_{\mathbf{i}}^{2/3}(1-\bar{\rho}_{\mathbf{i}}^{-1/3})\exp[\eta'(1-\bar{\rho}_{\mathbf{i}}^{-1/3})]-P_{\mathbf{i}}p_{\mathrm{h}} \tag{15}$$

The next question is that of the coupling. The density appears in Reynolds' equation (both one-dimensional and two-dimensional) in two places. Firstly it appears in the pressure flow term; however, in the region where the density will significantly deviate from unity, this term is not the dominant term in the equation. Consequently, its changes due to relaxing the density will not cause significant changes of the residual(s) of Reynolds' equation. Secondly it appears in the wedge term

$$\frac{\partial(\bar{\rho}H)}{\partial X} \tag{16}$$

Here it is more important, as this is the dominating term in the above-mentioned region. However, of the two variables appearing in it, the density is the less important one (from a relaxation point of view). Because of the global character of the elastic deformation integrals, the cumulative effect of pressure changes on the film thickness will be much larger than the changes in the density.

Summarising, it is concluded that changes induced when relaxing the density can be expected to affect the residuals of Reynolds' equation only in a moderate way. Hence, apart from appropriate linearization when relaxing Reynolds' equation, no special measures are needed and a straightforward extension of the relaxation scheme as outlined in Venner [15–17] can be expected to work. The resulting consecutive scheme is schematically drawn in Fig. 2, scheme A, where for the present case *relax lubricant model* stands for relaxing the density equation (in each grid point) once according to eqn. (14).

This relaxation process (with the force balance equation added to it as described in Lubrecht [1] and Venner

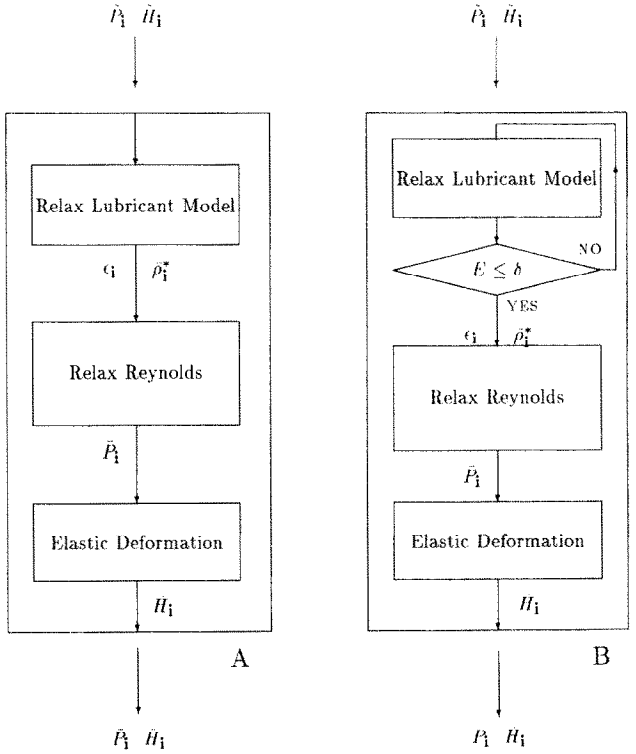

Fig. 2. Flow diagram of the relaxation process as proposed (scheme A), and the (computationally inefficient) alternative with a nested iterative loop (scheme B).

[15]) indeed can easily be shown to converge and smooth well for the full line- and circular-contact problems, even in highly loaded situations.

Next the incorporation of this relaxation in a multilevel solver is addressed. From a formal point of view an equation is added to the system. In multilevel solvers for non-linear problems it is essential that all equations are treated according to the so-called *FAS* rules; see p. 81 of Brandt [19]. Hence, in addition to the pressure and film thickness, now the density must be fully treated as a variable, *e.g.* transfer of residuals to the coarse grid and, when returning to the fine grid, it is corrected using the coarse grid result. These measures are essential for the convergence of the coarse grid correction cycle to be as fast as obtained for the closed-form density equation cases; see Venner [16]. Subsequently, multilevel multi-integration was introduced for the fast evaluation of the elastic deformation integrals, and the coarse grid correction cycle was incorporated in an *FMG* algorithm. Finally, the order of the approximation was raised as described in Venner [18].

Before shifting attention to results obtained with the algorithm described above, two final comments are appropriate. One might suggest that simply replacing every call for a density in the original algorithm by a number of iterations of the type of eqn. (14) can also do the job. This in effect is the same as the procedure followed so far when encountering coefficients determined by non-closed-form equations in a numerical solver for the pressure and film thickness, *e.g.* in the case where thermal and/or non-newtonian lubricant behaviour are taken into account. An "inner" iterative loop is introduced (in the lubricant model yielding the velocities and/or temperature, and thereby the coefficients ϵ_i in the discrete Reynolds equation) within the "outer" iterative loop for pressure and film thickness (which uses these coefficients). Such a scheme is schematically drawn in Fig. 2 and indicated as B.

Naturally if the scheme marked as A in Fig. 2 converges, scheme B also works. However, scheme B is inefficient from a computational point of view. The number of iterations to satisfy the error criterion for the inner loop should be sufficiently large to avoid slowdown of the convergence of the pressure and film thickness. This is particularly important when the speed of convergence of these latter variables is relatively large, as is characteristic of a multigrid algorithm (coarse grid correction cycle), and a single change per grid point as in the above algorithm is certainly not enough.

In the case of scheme B of Fig. 2, in the process of relaxing (and solving) a set of equations, a single equation (the lubricant model) is accurately (in practice often almost exactly) solved each sweep, even with pressure values still far away from the converged solution. This is done at the expense of many operations per grid point. Following the approach as outlined above, however, the variable associated with the additional equation, *i.e.* the density in the present case, converges along with the pressure and film thickness, in the same way (smooth components on coarse grids, etc.) and with the same speed at the computational cost of a single iteration per grid point visited in the solver.

The second comment to be made is that the analysis as given here also holds for more complex lubricant model extensions, *i.e.* non-newtonian lubricant behaviour or thermal effects. As long as Reynolds' equation is used, no matter how important these effects may be, they only effect Reynolds' equation via the coefficients in the pressure flow term and via an effective density in the wedge term. The coupling between Reynolds' equation and the film thickness equation via the elastic deformation integrals remains the strongest one in the entire system.

Hence, also for these cases a simple consecutive algorithm as drawn in Fig. 2, scheme A, allowing all variables (and thus the coefficients) to converge along with the pressure and the film thickness (on all grids) can be expected to work. It is stressed that, particularly for these model extensions, the alternative approach marked with B in Fig. 2 where the added equations are treated in an "inner" loop will become very costly in terms of computing time, as the added equations are differential and/or integral equations and thus more complex.

4. Results and discussion: line contact

Figure 3(a) shows the (dimensionless) pressure and (dimensionless) film thickness as a function of X for a moderately loaded line contact. The Moes dimensionless parameters for this case are $M=20$, $L=10$. In terms of the Dowson and Higginson parameters this load case can be given as $W=8.94\times10^{-5}$, $G=4730$, $U=1.0\times10^{-11}$. The maximum hertzian pressure for this case is 1.05 GPa. It has been used before as a reference case for a moderately loaded contact; see, for example Venner [15,18], where results obtained using the Dowson and Higginson density–pressure equation are discussed.

From Fig. 3(a) it is clear that using the Jacobson and Vinet density–pressure equation yields the same overall picture; an almost semi-elliptical pressure profile and a rather uniform film thickness in the central region. To reveal the effects of the increased compressibility on the solution requires a closer examination. Table 1 compares the (dimensionless) minimum and central film thickness for an incompressible lubricant, a lubricant compressible according to the Dowson–

TABLE 1. Dimensionless minimum (H_m) and central (H_c) film thickness as a function of the number of nodes for different compressibility equations. Line contact, $M=20$, $L=10$

Level	n	Incompressible		Compressible			
				Dowson Higginson		Jacobson Vinet	
		H_m	H_c	H_m	H_c	H_m	H_c
5	225	7.361×10^{-2}	9.771×10^{-2}	7.076×10^{-2}	8.242×10^{-2}	7.103×10^{-2}	7.912×10^{-2}
6	449	7.435×10^{-2}	9.885×10^{-2}	7.928×10^{-2}	8.367×10^{-2}	7.266×10^{-2}	7.993×10^{-2}
7	897	7.457×10^{-2}	9.913×10^{-2}	7.339×10^{-2}	8.392×10^{-2}	7.303×10^{-2}	8.016×10^{-2}
8	1793	7.466×10^{-2}	9.923×10^{-2}	7.354×10^{-2}	8.399×10^{-2}	7.316×10^{-2}	8.022×10^{-2}
9	3585	7.468×10^{-2}	9.923×10^{-2}	7.360×10^{-2}	8.400×10^{-2}	7.320×10^{-2}	8.023×10^{-2}
10	7169	7.468×10^{-2}	9.923×10^{-2}	7.363×10^{-2}	8.401×10^{-2}	7.321×10^{-2}	8.024×10^{-2}
11	14337	7.468×10^{-2}	9.923×10^{-2}	7.364×10^{-2}	8.401×10^{-2}	7.321×10^{-2}	8.024×10^{-2}
12	28673	7.468×10^{-2}	9.923×10^{-2}	7.364×10^{-2}	8.401×10^{-2}	7.321×10^{-2}	8.024×10^{-2}

Higginson equation and for the present result, *i.e.* when the Jacobson–Vinet equation is used. The central film thickness is defined as the film thickness H at the location where $\partial P/\partial X=0$, which for moderately to highly loaded contacts is the centre of the hertzian dry contact region $X=0$. In all cases the solution was computed on a domain $-4\leqslant X\leqslant 1.5$ with an *FMG* algorithm including double discretization (see Venner [18]), using 12 levels with 15 nodes on the coarsest grid.

Table 1 shows the values of the (dimensionless) minimum and central film thickness obtained on the eight finest levels. The results are presented in this way to show that the differences between the values of H_m and H_c obtained for the three situations can really be ascribed to the different compressibility equations and do not result from numerical errors.

Table 1 shows that the central film thickness is largest for an incompressible lubricant. Using the Dowson–Higginson equation it is about 15% smaller, and using the Jacobson–Vinet equation causes an additional 4% decrease. The minimum film thickness results show the same tendency; however, the absolute differences are much smaller, *i.e.* about 1%. The ratio of minimum to central film thickness differs accordingly; 1.33 for an incompressible lubricant, 1.14 using the Dowson and Higginson equation, and 1.10 using the Jacobson and Vinet equation.

Figure 3(b) shows the (dimensionless) film thickness profiles in the central region of the contact for the solutions listed in Table 1. This figure shows that, as was anticipated by Jacobson and Vinet, the compressibility equation mainly influences the film thickness in the central region. For an incompressible lubricant the film thickness in this region is virtually constant. Introducing compressibility into the system results in a smaller degree of uniformity; a local film thickness minimum shows up in the centre of the contact. With increasing compressibility this local minimum will become more pronounced and the value of the film thickness at this location will be smaller. This can be seen from comparing the graph obtained using the Dowson–Higginson equation with the one obtained using the Jacobson–Vinet equation.

The changes in the film thickness shown above can be traced back to Reynolds' equation. In the central region, owing to the high viscosity and small film thickness, the coefficient ϵ will be much smaller than unity. Hence, in this region the Poiseuille or pressure flow terms will be small compared to the wedge term, and eqn. (1) reduces to:

$$\frac{\mathrm{d}(\bar{\rho}H)}{\mathrm{d}X}\approx 0 \tag{17}$$

See also Venner [15,16]. As a result, the following equation

$$\bar{\rho}H\approx c \tag{18}$$

holds in the central region, where the constant c is the product of $\bar{\rho}$ and H at the entrance of the high-viscosity region, *i.e.* near $X=-1$. In the incompressible case, $\bar{\rho}=1$; hence the film thickness in the central region will tend to be constant. However, in the compressible case an increase of the density must be matched by a decrease in the film thickness. Bearing in mind the roughly hertzian pressure profile in the central region (smooth surfaces), this must indeed lead to the previously mentioned local minimum in the film thickness at $X=0$. Obviously, the total reduction of the film thickness in the region where eqn. (17) holds and $X<0$ is directly coupled to the increase of the density with the pressure. Hence, for a higher compressibility it will be larger, as is indeed shown by the results.

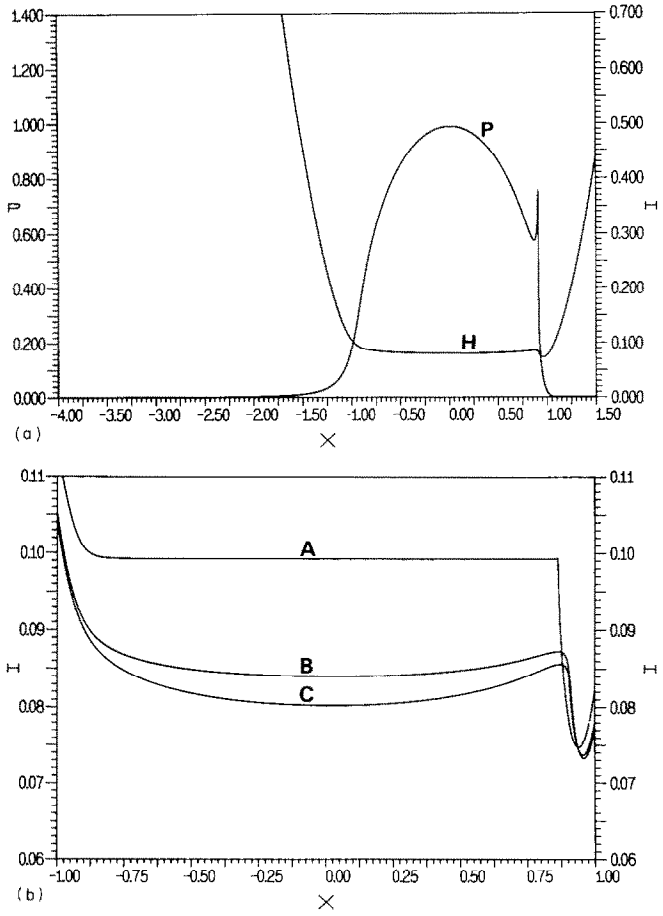

Fig. 3. (a) Dimensionless pressure P and film thickness H as a function of X for $M=20$ and $L=10$, computed using the Jacobson and Vinet relation. (b) Dimensionless film thickness H as a function of X in the central region of the contact for an incompressible lubricant (curve A), for compressibility according to the Dowson and Higginson equation (curve B) and for compressibility according to the Jacobson and Vinet equation (curve C) ($M=20$ and $L=10$).

However, a much stronger statement can be made. The constant c in eqn. (18) is determined by the total mass flow through the contact. Since the conditions in the inlet for the compressible and incompressible situation are hardly different, *i.e.* low pressures, so $\bar{\rho}$ very close to unity, the mass flow through the contact for both cases cannot differ much. As a result c for both cases will be almost the same. Consequently, from applying eqn. (18) at $X=0$ for both cases, it follows that by approximation:

$$\frac{H_c^i}{H_c^c} = \bar{\rho}_c \tag{19}$$

where the superscript i stands for incompressible and the superscript c for compressible. $\bar{\rho}_c$ denotes the density at $X=0$ for the compressible case, which for a moderately to highly loaded contact is simply $\bar{\rho}(p_h)$.

With the present set of results, eqn. (19) can easily be verified. For this load case, $p_h=1.05$ GPa. This gives $\bar{\rho}_c=1.21$ for the Dowson–Higginson equation and $\bar{\rho}_c=1.27$ for the Jacobson–Vinet equation. With these values and H_c^i from Table 1, eqn. (19) predicts $H_c=8.2\times10^{-2}$ for Dowson and Higginson compressibility and $H_c=7.8\times10^{-2}$ if the Jacobson and Vinet equation is used. Comparing these predictions with the values obtained from the full numerical solutions the difference is less than 3%!

As a next case we consider a highly loaded example. The Moes dimensionless parameters for this case are $M=200$ and $L=10$, conditions we used as a reference high load case before; for example, see Venner [15,18]. In terms of the Dowson and Higginson dimensionless parameters it may be expressed as $W=8.94\times10^{-4}$, $G=4730$, and $U=1.0\times10^{-11}$. For this case the maximum hertzian pressure is 3.3 GPa. Figure 4(a) shows the pressure profile and film thickness obtained using

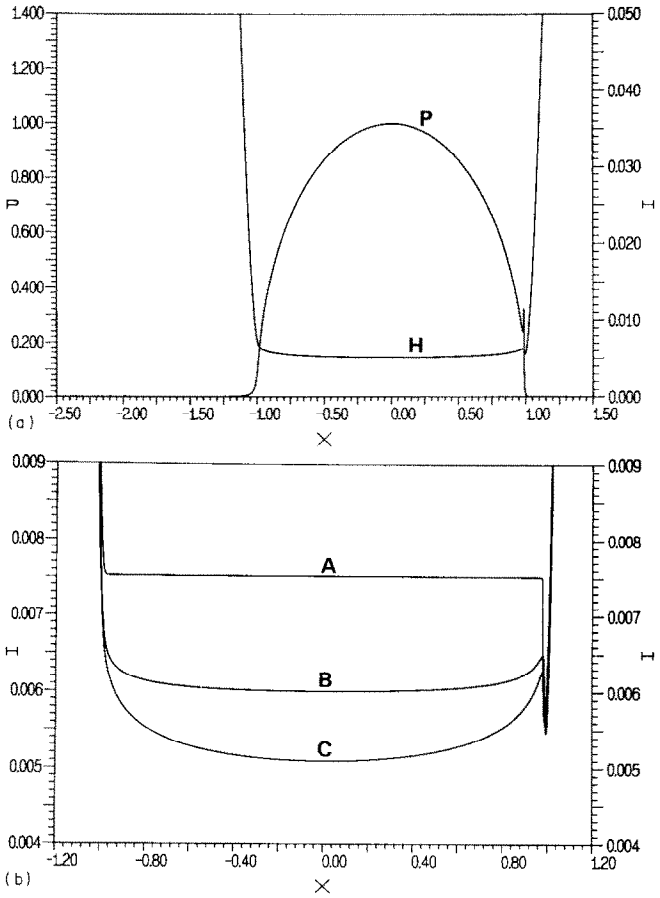

Fig. 4. (a) Dimensionless pressure P and film thickness H as a function of X for $M=200$ and $L=10$ computed using the Jacobson and Vinet equation. (b) Dimensionless film thickness H as a function of X in the central region of the contact for an incompressible lubricant (curve A), for compressibility according to the Dowson and Higginson equation (curve B) and for compressibility according to the Jacobson and Vinet equation (curve C) ($M=200$ and $L=10$).

the Jacobson–Vinet density–pressure equation. The solution was computed using an *FMG* algorithm with 13 levels and double discretization on a domain $-2.5 \leqslant X \leqslant 1.5$. Table 2 shows the values of the dimensionless minimum and central film thickness obtained from the fifth level onwards. In addition, this table gives the values of these parameters obtained for an incompressible lubricant and when the Dowson–Higginson equation is used. Furthermore, Fig. 4(b) gives the film thickness profile in the central region for the three cases.

Going from an incompressible lubricant to compressibility according to Dowson and Higginson, the results show the same tendency as for the previous load case, *i.e.* a noticeable decrease of the central film thickness, and a minimum film thickness that is only slightly smaller. In both cases the minimum film thickness occurs at the end of the central region, *i.e.* near $X=1$. However, introducing compressibility according to the Jacobson and Vinet equation significantly changes this picture, *i.e.* the density increase in the central region is so large that the local film thickness minimum at the centre drops below the local minimum near $X=1$. Hence, the overall minimum film thickness does not occur at its usual location near the end of the hertzian contact region but in the centre instead. Consequently its value is significantly different from the overall minimum film thickness for an incompressible lubricant or when the Dowson and Higginson equation is used. For the conditions considered it is some 8% smaller. The ratio of minimum to central film thickness is affected accordingly. For the incompressible case it is 1.33, with compressibility according to Dowson and Higginson it is 1.09 and for the present case it (obviously) equals one.

As for the moderately loaded case above, the predictions of eqn. (19) closely match the numerical results. Here $p_h = 3.3$ GPa, which gives $\bar{\rho}_c = 1.29$ with the Dowson and Higginson equation and $\bar{\rho}_c = 1.52$ with the Jacobson and Vinet equation. With these values and H_c^i from Table 2, eqn. (19) predicts $H_c = 5.83 \times 10^{-3}$ for the Dowson and Higginson case and $H_c = 4.95 \times 10^{-3}$ for the Jacobson and Vinet result; values that differ from the numerical results by less than 3%.

The theoretical analysis presented in this section resulted in a very simple relation between the change of the central film thickness due to compressiblity and the density in the centre of the contact *that will hold for moderately to highly loaded contacts*. This relation was confirmed by the numerical results. The resulting equation, *i.e.* eqn. (19), allows straightforward prediction of the central film thickness for any compressibility equation if the value for the incompressible case is known. Furthermore, because the film thickness in the local minimum at the end of the central region (the usual minimum film thickness) is only slightly influenced by compressibility, the minimum film thickness in the compressible case can be predicted by

$$H_m^c = \min(H_c^c, H_m^i) \tag{20}$$

This equation reflects what was shown in the numerical results, *i.e.* that compressibility can cause the minimum film thickness in a moderately to highly loaded contact to occur at the centre of the contact instead of in the exit region. The question now arises of the conditions (load conditions, density–pressure equation) under which one would expect this to happen. This will be investigated below.

Again the argument assumes that for moderately to highly loaded contacts the local film minimum near $X=1$ is insensitive to compressibility. As a result, a minimum requirement for the minimum and central film thickness in the compressible case to be equal is

TABLE 2. Dimensionless minimum (H_m) and central (H_c) film thickness as a function of the number of nodes for different compressibility equations. Line contact, $M=200$, $L=10$

Level	n	Incompressible		Compressible			
		H_m	H_c	Dowson Higginson		Jacobson Vinet	
				H_m	H_c	H_m	H_c
5	225	3.547×10^{-3}	5.435×10^{-3}	4.281×10^{-3}	4.484×10^{-3}	3.767×10^{-3}	3.676×10^{-3}
6	449	5.119×10^{-3}	6.985×10^{-3}	5.011×10^{-3}	5.649×10^{-3}	4.789×10^{-3}	4.789×10^{-3}
7	897	5.506×10^{-3}	7.393×10^{-3}	5.410×10^{-3}	5.908×10^{-3}	5.008×10^{-3}	5.008×10^{-3}
8	1793	5.585×10^{-3}	7.488×10^{-3}	5.466×10^{-3}	5.979×10^{-3}	5.069×10^{-3}	5.069×10^{-3}
9	3585	5.609×10^{-3}	7.513×10^{-3}	5.502×10^{-3}	5.998×10^{-3}	5.086×10^{-3}	5.086×10^{-3}
10	7169	5.625×10^{-3}	7.520×10^{-3}	5.512×10^{-3}	6.003×10^{-3}	5.090×10^{-3}	5.090×10^{-3}
11	14337	5.618×10^{-3}	7.521×10^{-3}	5.516×10^{-3}	6.004×10^{-3}	5.091×10^{-3}	5.091×10^{-3}
12	28673	5.612×10^{-3}	7.521×10^{-3}	5.517×10^{-3}	6.005×10^{-3}	5.091×10^{-3}	5.091×10^{-3}
13	57345	5.610×10^{-3}	7.521×10^{-3}	5.518×10^{-3}	6.005×10^{-3}	5.091×10^{-3}	5.091×10^{-3}

$$\bar{\rho}_c \approx \bar{\rho}(p_h) > \frac{H_c^i}{H_m^i} \tag{21}$$

Now it is well known that for the incompressible line contact the ratio between minimum and central film thickness is roughly constant at 4/3. Obviously when using the Dowson and Higginson equation there is no p_h for which $\bar{\rho}(p_h)$ can really exceed this value. Hence, the above situation will not occur, and indeed to the authors' knowledge has not been reported. However, when using the Jacobson and Vinet equation, $\bar{\rho}(p_h)$ can exceed this value. For the given values of η' and B_0 this happens for $p_h \approx 1.5$ GPa. So, using this relation, the minimum film thickness can be expected to occur in the centre of the contact if p_h significantly exceeds 1.5 GPa. In a similar way an estimate of the load beyond which this phenomenon can be expected to occur can be obtained for any other proposed density–pressure equation.

5. Results and discussion: circular contact

Next we consider the circular-contact problem. The solution algorithm explained in Venner [18] was extended as described in Section 3 and some results are presented here. As in the previous case, moderately and highly loaded contact conditions are considered. The Moes dimensionless parameters describing the first load situation are $M=50$ and $L=10$. Results for this load situation obtained using the Dowson and Higginson density–pressure equation have appeared in Venner [17,18]. In terms of the Dowson and Hamrock [20] dimensionless parameters, it may be presented as $W=4.73\times10^{-7}$, $G=4730$, and $U=1.0\times10^{-11}$. With $\alpha=1.7\times10^{-8}$ the maximum hertzian pressure is 0.79 GPa.

Figures 5(a) and 5(b) show the dimensionless pressure and the associated dimensionless film thickness obtained using the Jacobson and Vinet equation. The solution was computed on a uniform grid with 513×513 nodes covering the domain $\{(X,Y)\in\mathbb{R}^2 | -4.5\leqslant X\leqslant 1.5 \wedge -3\leqslant Y\leqslant 3\}$, using an *FMG* algorithm with double discretization, see Venner [18].

Because compressibility is not one of the dominant film formation mechanisms, as in the line-contact case, at first sight the solution hardly differs from the solution obtained using the Dowson and Higginson equation, and it shows all well-known features of two-dimensional EHL; a pressure profile in the inlet gradually building up to a semi-ellipsoid, with the pressure spike region preceding the cavitated zone. The film thickness shows a rather uniform region in the centre of the contact with a decrease to both sides, yielding what is generally referred to as the side lobes. (Note the reversal of the vertical axis in Fig. 5(b).)

To reveal the effect of the higher compressibility following from the use of the Jacobson and Vinet density–pressure equation, again a closer examination is needed. Table 3 gives the (dimensionless) minimum and central film thickness as a function of the mesh size for three situations: incompressible, compressibility according to the Dowson and Higginson equation and compressibility according to the Jacobson and Vinet equation. The central film thickness is defined as the film thickness H at the location where $\partial P/\partial X=0$ and $\partial P/\partial Y=0$, which, for moderately to highly loaded contacts, is the centre of the contact ($X=0, Y=0$). Secondly, Fig. 5(c) shows the film thickness contour plot for these three situations. All solutions were calculated as described above using the same domain.

From Table 3 it can be seen that, as in the line-contact case, the main effect of the higher compressibility is on the central film thickness. Compared to the incompressible result, introducing compressibility with the Dowson and Higginson equation yields a 14% lower value, and the larger compressibility due to the use of the Jacobson and Vinet equation results in an additional reduction of 2.5%. The differences between the minimum film thickness for the three cases are much smaller, *e.g.* the use of the Dowson and Higginson relation yields a minimum film thickness that is 4% smaller than it is in the incompressible case, and using the Jacobson and Vinet equation only gives an additional 1% decrease. The ratio of central to minimum film thickness changes accordingly, *i.e.* 1.86 in the incompressible case, 1.62 in the compressible case with the Dowson and Higginson equation and 1.60 when the Jacobson and Vinet equation is used.

Note that Table 3 also shows that these observed differences (in central and minimum film thickness) can indeed with confidence be ascribed to the different compressibility equations, as they are much larger than the numerical error in the values, which, for both the minimum and the central film thickness, is smaller than 0.1%. (This can be estimated from the convergence history shown by the results on the different levels.)

The fact that the use of different compressibility relations predominantly influences the film thickness in the central region is most clearly reflected in a film thickness contour plot. Figure 5(c) shows such a plot for the solutions listed in Table 3.

The film thickness changes discussed above can be explained from Reynolds' equation. As in the line-contact case (see Section 4), the two-dimensional Reynolds equation, *i.e.* eqn. (7), in the central region reduces to:

$$\frac{\partial(\bar{\rho}H)}{\partial X} \approx 0 \tag{22}$$

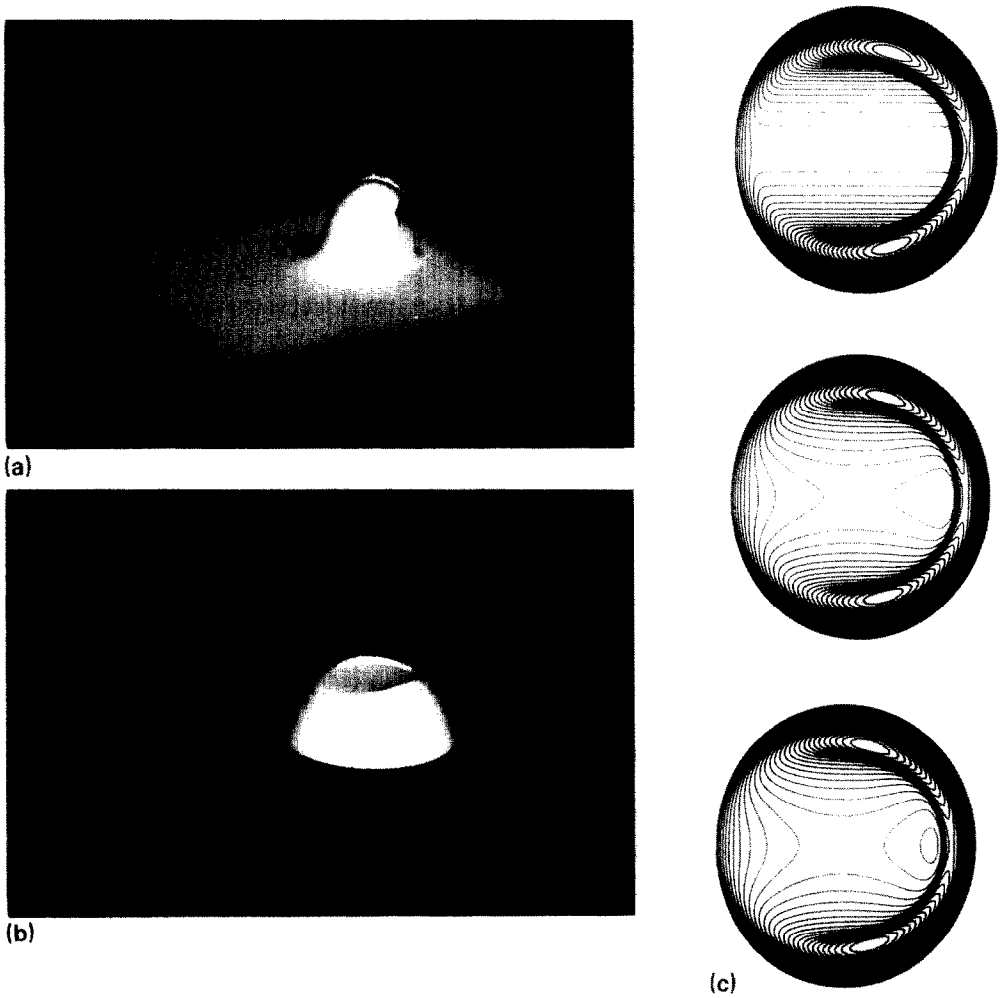

Fig. 5. (a) Circular contact: dimensionless pressure P as a function of X and Y for $M=50$ and $L=10$, computed using the Jacobson and Vinet relation. (b) Circular contact: dimensionless film thickness H as a function of X and Y for $M=50$ and $L=10$, computed using the Jacobson and Vinet relation. (c) Contour plot of the dimensionless film thickness H for an incompressible lubricant (top), for compressibility according to the Dowson and Higginson equation (centre) and for compressibility according to the Jacobson and Vinet equation (bottom). ($\Delta H=5.0\times10^{-3}$, $M=50$ and $L=10$.)

TABLE 3. Dimensionless minimum (H_m) and central (H_c) film thickness as a function of the number of nodes for different compressibility equations. Circular contact, $M=50$, $L=10$

Level	n	Incompressible		Compressible			
		H_m	H_c	Dowson Higginson		Jacobson Vinet	
				H_m	H_c	H_m	H_c
3	33×33	1.338×10^{-1}	2.762×10^{-2}	1.310×10^{-1}	2.264×10^{-1}	1.285×10^{-1}	2.117×10^{-1}
4	65×65	1.587×10^{-1}	2.916×10^{-1}	1.523×10^{-1}	2.506×10^{-1}	1.534×10^{-1}	2.437×10^{-1}
5	129×129	1.628×10^{-1}	2.971×10^{-1}	1.569×10^{-1}	2.554×10^{-1}	1.559×10^{-1}	2.479×10^{-1}
6	257×257	1.642×10^{-1}	2.995×10^{-1}	1.583×10^{-1}	2.573×10^{-1}	1.571×10^{-1}	2.498×10^{-1}
7	513×513	1.645×10^{-1}	3.004×10^{-1}	1.586×10^{-1}	2.580×10^{-1}	1.574×10^{-1}	2.505×10^{-1}

Note that this indicates that the flow in the central region is unidirectional (no flow in Y direction). From eqn. (22) it follows that the product of density and film thickness will tend to remain constant along a line of constant Y:

$$\bar{\rho}H\approx c(Y) \tag{23}$$

In the case of an incompressible lubricant $\bar{\rho}=1$ so $H\approx c(Y)$ which, as the figure shows, results in straight

lines in the central region of the film thickness contour plot. However, in the case of a compressible lubricant $\bar{\rho}H$ will tend to be constant along a line of constant Y, so, in regions on this line where the pressure increases, the density increases, and consequently the film thickness will decrease. Hence, on such a line of constant Y, the film thickness will show a local minimum at $X=0$. For the entire contour plot this implies that in the central region the contour lines will not be straight as above, but concave with respect to the central line $Y=0$. Increasing the compressibility enhances this phenomenon as can be seen from Fig. 5(c) by comparing the film thickness contour plot in the centre with the one at the bottom.

For the point contact, a similar argument as given in the previous section for a line contact holds, *i.e.* $c(Y)$ is determined by the (local) mass flow in the inlet, *i.e.* near $X^2+Y^2=1$ with $X<0$, and, as the conditions in the inlet for the compressible and incompressible case are virtually the same, $c(Y)$ must be almost the same for both situations. Subsequently from applying eqn. (23) to the centre of the contact ($X=0$, $Y=0$) (the location of the central film thickness), it follows that for moderately to highly loaded point contacts

$$\frac{H_c^i}{H_c^c}=\bar{\rho}_c \tag{24}$$

can be expected to hold. This is the correlation reported by Kweh *et al.* [3]. It also shows quite clearly in the present numerical results. For this load case, $p_h=0.79$ GPa. Hence, $\bar{\rho}_c=1.20$ using the Dowson and Higginson equation and $\bar{\rho}_c=1.23$ using the Jacobson and Vinet equation. With these values, and the central film thickness for the incompressible case from Table 3, eqn. (24) predicts $H_c=0.25$ for the Dowson and Higginson case and $H_c=0.24$ for the Jacobson and Vinet case, which, again, accurately reflects the changes observed between the different numerical solutions.

The values of the Moes dimensionless parameters for the second (more highly) loaded condition are $M=1000$ and $L=10$. This case was used as a typical highly loaded contact before, for example, see Venner [18] but then using the Dowson and Higginson equation. It may be expressed in the Dowson and Hamrock [20] parameters by: $W=9.46\times10^{-6}$, $U=1.0\times10^{-11}$ and $G=4730$ and, assuming $\alpha=1.7\times10^{-8}$, the maximum hertzian pressure for this case is about 2 GPa.

Figures 6(a) and 6(b) show the (dimensionless) pressure and film thickness as a function of X and Y obtained when the Jacobson and Vinet relation is used. The solution was obtained on a uniform grid covering the domain $\{(X,Y)\in\mathbb{R}^2 | -2.5\leqslant X\leqslant 1.5 \wedge -2\leqslant Y\leqslant 2\}$. Table 4 shows the (dimensionless) minimum and central film thickness as a function of the mesh size on the finest four grids used in the *FMG* algorithm. Besides, the values obtained for the same load case, assuming an incompressible lubricant and with the Dowson and Higginson equation, are listed.

Table 4 shows that for this highly loaded case the effects of the compressibility are basically the same as for the previous load condition, *i.e.* the central film thickness decreases noticeably, whereas the minimum film thickness is hardly affected. In fact, the differences between the minimum film thickness for the three cases are so small that they are only slightly larger than the numerical error, which is about 1%. Again these changes are reflected in the ratio between central and minimum film thickness, which is 3.3 for the incompressible case, 2.8 using the Dowson and Higginson equation, and 2.6 using the Jacobson and Vinet equation.

Figure 6(c) shows the film thickness contour plots for all three cases. These plots show even more strongly the differences discussed before, *i.e.* straight lines for an incompressible lubricant and with increasing compressibility contour lines increasingly concave with respect to the central axis.

Furthermore, as for the previous load case the present results validate the analysis leading to eqn. (24). For this case $p_h=2.14$ GPa: hence $\bar{\rho}_c=1.27$ using the Dowson and Higginson equation and $\bar{\rho}_c=1.42$ using the Jacobson and Vinet equation. With these values and the central film thickness for the incompressible case from Table 4, eqn. (24) predicts $H_c=2.76\times10^{-2}$ for the Dowson and Higginson case and $H_c=2.50\times10^{-2}$ for the Jacobson and Vinet case.

In the previous section it was observed that for a sufficiently highly loaded line contact, owing to the compressibility the minimum film thickness occurred in the centre of the contact. However, in the present circular-contact case, in spite of the high load this phenomenon does not occur, and the central film thickness remains much larger than the minimum film thickness. The question arises of whether a compressibility-induced minimum film thickness in the centre of the contact can occur at all in a circular contact.

Kweh *et al.* [3] and the present results show that the (local) minimum film thickness in the side lobes is quite insensitive to compressibility effects. Hence, as in the line contact

$$\bar{\rho}(p_h)>\frac{H_c^i}{H_m^i} \tag{25}$$

can be taken as a requirement for the minimum film thickness in the compressible case to occur in the centre of the contact. Now, unlike the incompressible line-contact case, the ratio of central to minimum film thickness is not constant. For the conditions considered, *i.e.* moderately to highly loaded contacts, the minimum film thickness normally occurs in the side lobes. With increasing load these sidelobes move outwards, and the ratio of minimum to central film thickness increases

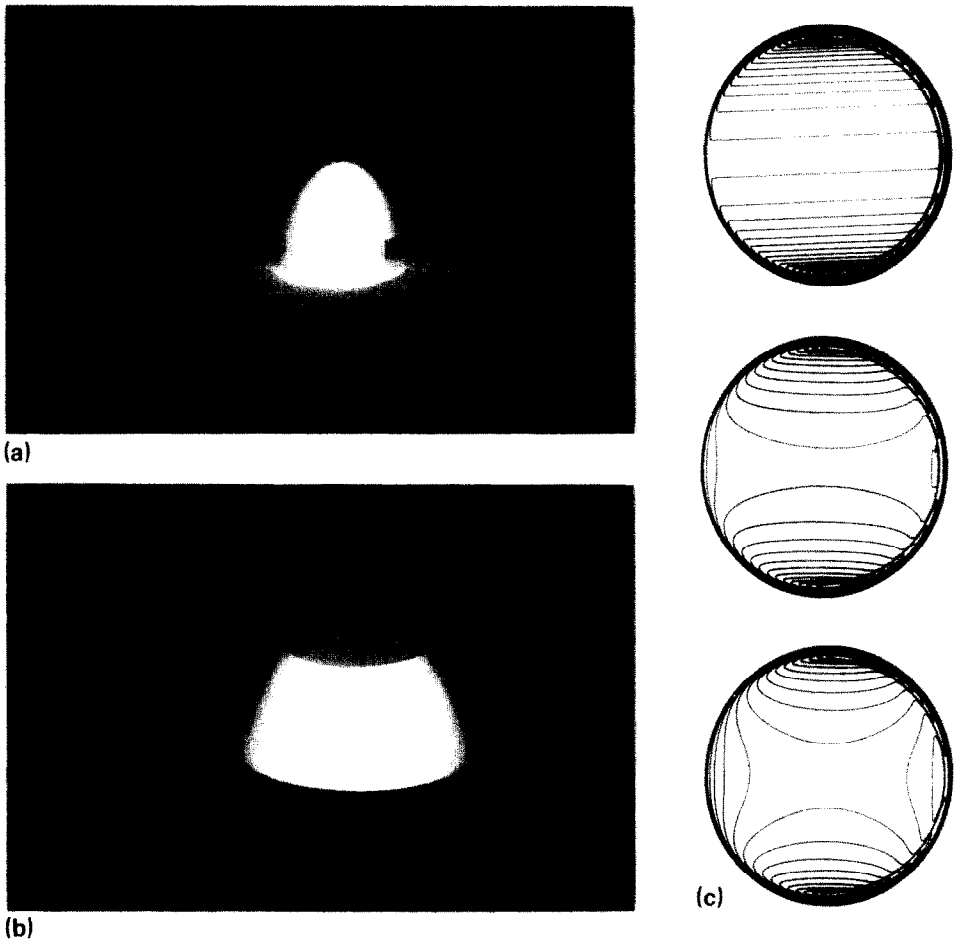

Fig. 6. (a) Circular contact: dimensionless pressure P as a function of X and Y for $M=1000$ and $L=10$, computed using the Jacobson and Vinet relation. (b) Circular contact: dimensionless film thickness H as a function of X and Y for $M=1000$ and $L=10$, computed using the Jacobson and Vinet relation. (c) Contour plot of the dimensionless film thickness H for an incompressible lubricant (top), for compressibility according to Dowson and Higginson (centre) and for compressibility according to Jacobson and Vinet (bottom) ($\Delta H=1.5\times10^{-3}$, $M=1000$ and $L=10$).

TABLE 4. Dimensionless minimum (H_m) and central (H_c) film thickness as a function of the number of nodes for different compressibility equations. Circular contact, $M=1000$, $L=10$

Level	n	Incompressible		Compressible			
		H_m	H_c	Dowson Higginson		Jacobson Vinet	
				H_m	H_c	H_m	H_c
4	65×65	2.142×10^{-3}	2.497×10^{-2}	1.927×10^{-3}	1.747×10^{-2}	2.067×10^{-3}	1.563×10^{-2}
5	129×129	8.831×10^{-3}	3.213×10^{-2}	8.246×10^{-3}	2.638×10^{-2}	8.131×10^{-3}	2.364×10^{-2}
6	257×257	1.020×10^{-2}	3.438×10^{-2}	9.772×10^{-3}	2.773×10^{-2}	9.605×10^{-3}	2.491×10^{-2}
7	513×513	1.065×10^{-2}	3.510×10^{-2}	1.006×10^{-2}	2.825×10^{-2}	9.904×10^{-3}	2.532×10^{-2}

with load, as is clearly shown in Kweh *et al.* [3], Venner [15] and Lubrecht [1]. This behaviour reflects one of the fundamental differences between line and point contacts resulting from the additional dimension. Based on the results presented in Venner [15] (converted assuming $H^i_m=H^c_m$ and using eqn. (24)), for sufficiently large M the ratio H^i_c/H^i_m can be approximated by:

$$\frac{H^i_c}{H^i_m}=C_L M^{2/9} \tag{26}$$

where $C_L=C(L)$, For example, $C_{10}\approx0.76$, as can be checked using the results presented in this section. Now let $\bar{\rho}$ be approximated by

$$\bar{\rho}=1+C_d p^{\gamma} \tag{27}$$

with C_d and γ known constants, then

$$\bar{\rho}_c=1+C_d(p_h)^{\gamma} \tag{28}$$

In a circular contact

$$p_h=\frac{L}{\alpha\pi}\left(\frac{3M}{2}\right)^{1/3} \tag{29}$$

hence

$$\bar{\rho}_c=1+C'_d L^{\gamma}(M)^{\gamma/3} \tag{30}$$

Assuming M to be large, for the situation of interest to occur, *i.e.* for the central film thickness to drop below the (local) minimum in the side lobes beyond a certain load, at least

$$\gamma>2/3 \tag{31}$$

Clearly the Dowson and Higginson equation does not satisfy this condition, as it approaches a limit with increasing load. However, the Jacobson and Vinet equation also does not satisfy the condition of eqn. (31). It can be shown that, for the values of B_0 and η' considered, the density according to this equation (up to pressures far beyond realistic ones) closely satisfies eqn. (27), with $C_d=9.1\times10^{-11}$, and $\gamma=1/2$. Consequently the density does not increase fast enough with pressure for eqn. (25) to become true and therefore, in the authors' opinion, a compressibility-induced minimum film thickness in the centre is very unlikely to occur in a circular contact.

Indeed, so far we have not observed it in numerical simulations of the circular contact. For example, Fig. 7 shows the film thickness contour plot for the load case $M=2000$, $L=10$, when the Jacobson and Vinet equation is used. This load case may be expressed in the Dowson and Hamrock [20] parameters by $W=1.89\times10^{-5}$, $U=1.0\times10^{-11}$ and $G=4730$. With $\alpha=1.7\times10^{-8}$, the maximum hertzian pressure for this case is about 2.7 GPa. From the figure it is clear that there is still a significant difference between minimum and central film thickness. In fact, for this case $H_c/H_m=3.0$, *i.e.* larger than $H_c/H_m=2.6$ found above for the conditions $M=1000$ and $L=10$, see Table 4.

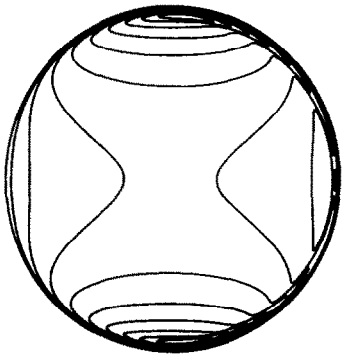

Fig. 7. Contour plot of the dimensionless film thickness H for a lubricant compressible according to the Jacobson and Vinet equation ($\Delta H=1.5\times10^{-3}$, $M=2000$ and $L=10$).

6. Conclusion

For study of the effects of compressibility on the film thickness and as a first step to incorporating lubricant behaviour that yields non-closed-form coefficients in Reynolds' equation, this paper describes the efficient incorporation of the Jacobson and Vinet density–pressure equation in a multilevel solver for the pressure and film thickness in an EHL line- and point-contact problem.

For different load conditions, the results obtained with this equation were compared with the results obtained assuming an incompressible lubricant and with results obtained using the commonly applied Dowson and Higginson density–pressure relation. Both line- and circular-contact results were discussed. It was shown that, although compressibility is not one of the predominant effects accounting for film formation, it does determine to a great extent the shape of the lubricant film in the central region of the contact. Consequently, different compressibility equations may have some interesting consequences. For example, it was shown that, in the highly loaded line-contact problem using the Jacobson and Vinet equation, situations can arise where (unlike the usual situation) the minimum film thickness occurs in the centre of the contact and not at the exit. This phenomenon was not observed in circular-contact results.

The observed effects were explained from an analysis of Reynolds' equation. Firstly this analysis yielded a formula accurately predicting the effect of the compressibility on the central film thickness in moderately to highly loaded contacts, once the incompressible result is known. Secondly it enabled investigation of the previously mentioned phenomenon of a compressibility-induced minimum film thickness in the centre of the contact, and showed it to be very unlikely to occur in a circular contact, owing to the strongly increasing ratio between central and minimum film thicknesses in such contacts.

With respect to two-dimensional EHL, we restricted ourselves to the circular contact, as it contains all essential elements of two-dimensional EHL. However, most "real life" contacts are elliptical. Note that eqns. (22) and (23) in Section 5 also apply to such contacts. Hence, eqn. (24) describes the film thinning due to compressibility *regardless of the type of contact — line, elliptical or circular* — and similarly the condition of

eqn. (25) holds as a minimum requirement for a compressibility-induced overall minimum film thickness in the centre regardless of the type of contact.

Now whether indeed such an overall minimum in the centre can occur in an elliptical contact for practical (moderate to high) loading cases remains to be investigated, as a final conclusion requires extensive results giving the location of the minimum film thickness, and the ratio between minimum and central film thicknesses as a function of the load parameters and ellipticity ratio. On the one hand, based on the line-contact results, one may expect the phenomenon (overall minimum film thickness in the centre of the contact) to occur for highly loaded wide elliptical contacts. On the other hand, as in circular contacts, also in elliptical contacts the minimum film thickness for moderate to high loads quite often occurs in the side lobes, and the ratio H_c^i/H_m^i changes with load and ellipticity ratio. Now, only if $\bar{\rho}(p_h)$ increases faster with the load and the ellipticity ratio than H_c^i/H_m^i can a compressibility-induced overall minimum in the centre occur.

Acknowledgments

The authors gratefully acknowledge the support of the Royal Netherlands Academy of Arts and Sciences and the Technology Foundation STW.

References

1 A.A. Lubrecht, The numerical solution of the elastohydrodynamically lubricated line and point contact problem using multigrid techniques, *Ph.D. Thesis*, University of Twente, Enschede, 1987, ISBN 90-9001583-3.
2 B.J. Hamrock, P. Pan and R.T. Lee, Pressure spikes in elastohydrodynamically lubricated conjunctions, *ASME J. Tribol., 110* (1988) 279–284.
3 C.C. Kweh, H.P. Evans and R.W. Snidle, Elastohydrodynamic lubrication of heavily loaded circular contacts, *Proc. Inst. Mech. Eng., 203* (1989) 133–148.
4 D. Dowson and G.R. Higginson, *Elasto-hydrodynamic Lubrication, The Fundamentals of Roller and Gear Lubrication*, Pergamon Press, Oxford, UK, 1966.
5 B.O. Jacobson and P. Vinet, A model for the influence of pressure on the bulk modulus and the influence of temperature on the solidification pressure for liquid lubricants, *ASME J. Tribol., 109* (1987) 709–714.
6 K.T. Ramesh, The short-time compressibility of elastohydrodynamic lubricants, *ASME J. Tribol., 113* (1991) 361–371.
7 P.R. Yang and S.Z. Wen, A generalized Reynolds equation for non-newtonian thermal elastohydrodynamic lubrication, *ASME J. Tribol., 112* (1990) 631–636.
8 C.J.A. Roelands, Correlational aspects of the viscosity–temperature–pressure relationship of lubricating oils, *Ph.D. Thesis*, Technische Hogeschool Delft, Netherlands, 1966, published by V.R.B., Groningen, Netherlands.
9 A.A. Lubrecht, W.E. ten Napel and R. Bosma, Multigrid, an alternative method for calculating film thickness and pressure profiles in elastohydrodynamically lubricated line contacts, *ASME J. Tribol., 108* (1986) 551–556.
10 A.A. Lubrecht, W.E. ten Napel and R. Bosma, Multigrid, an alternative method of solution for two-dimensional elastohydrodynamically lubricated point contact calculations, *ASME J. Tribol., 109* (1987) 437–443.
11 K.F. Osborn and F. Sadeghi, Time dependent line EHD lubrication using the multigrid/multilevel technique, *ASME J. Tribol., 114* (1992) 68–74.
12 K.H. Kim and F. Sadeghi, Non-newtonian EHL of point contact, *ASME J. Tribol., 113* (1991) 703–709.
13 X. Ai and H.S. Cheng, A transient EHL analysis for line contacts with measured surface roughness using multigrid technique, submitted for publication.
14 C. Huang, S.Z. Wen and P. Huang, Multilevel solution of the elastohydrodynamic lubrication of concentrated contacts in spiroid gears, *ASME J. Tribol.*, in press; also ASME preprint 92-TRIB-17, ASME/STLE Tribology Conf., San Diego, CA, October 18–21, 1992.
15 C.H. Venner, Multilevel solution of the EHL line and point contact problems, *Ph.D. Thesis*, University of Twente, Enschede, Netherlands, 1991, ISBN 90-9003974-0.
16 C.H. Venner, W.E. ten Napel and R. Bosma, Advanced multilevel solution of the ehl line contact problem, *ASME J. Tribol., 112* (1990) 426–432.
17 C.H. Venner and W.E. ten Napel, Advanced multilevel solution of the EHL circular contact problem, Part I: Theoretical formulation and algorithm, *Wear, 152* (1992) 351–367.
18 C.H. Venner, Higher order multilevel solvers for the EHL line and point contact problem, submitted for publication in *ASME J. Tribol.*; also internal report WB92-TR203, Department of Mechanical Engineering, University of Twente, Enschede, Netherlands, 1993.
19 A. Brandt, *1984 Multigrid Techniques: 1984 Guide with applications to Fluid Dynamics, GMD Studien No. 85*, Gesellschaft für Mathematik und Datenverarbeitung MBH, Bonn, Germany, 1984.
20 B.J. Hamrock and D. Dowson, Isothermal elastohydrodynamic lubrication of point contacts, Part III, Fully flooded results, *ASME J. Tribol., 99* 264–276.

Appendix: Nomenclature

a	radius hertzian contact circle (2-D), $a=[(3FR_x)/(2E')]^{1/3}$
b	half-width hertzian contact (1-D), $b=[(8wR)/(\pi E')]^{1/2}$
B_0	lubricant parameter in density–pressure equation
c	constant
C_d	constant
C'_d	constant
C_L	constant, value depending on L
E	modulus of elasticity
E'	reduced modulus of elasticity, $2/E'=(1-\nu_1^2)/E_1+(1-\nu_2^2)/E_2$
F	external load (2-D)
G	material parametcr, $G=\alpha E'$
$\bar{h}$	film thickness

H dimensionless film thickness
(1-D), $H=\bar{h}R/b^2$
(2-D), $H=\bar{h}R_x/a^2$
H_0 integration constant
L dimensionless materials parameter (Moes)
(1-D), $L=G(2U)^{1/4}$
(2-D), $L=G(2U)^{1/4}$
M dimensionless load parameter (Moes)
(1-D), $M=W(2U)^{-1/2}$
(2-D), $M=W(2U)^{-3/4}$
n number of nodes on grid
p pressure
p_h maximum hertzian pressure
(1-D), $p_h=(2w)/(\pi b)$
(2-D), $p_h=(3F)/(2\pi a^2)$
P dimensionless pressure, $P=p/p_h$
r residual
R reduced radius of curvature
(1-D), $R^{-1}=R_1^{-1}+R_2^{-1}$
R_x reduced radius of curvature in x direction
(2-D), $R_x^{-1}=R_{1x}^{-1}+R_{2x}^{-1}$
R_y reduced radius of curvature in y direction
(2-D), $R_y^{-1}=R_{1y}^{-1}+R_{2y}^{-1}$
u_s sum velocity, $u_s=u_1+u_2$
U dimensionless speed parameter
(1-D), $U=(\eta_0 u_s)/(2E'R)$
(2-D), $U=(\eta_0 u_s)/(2E'R_x)$
w load per unit width (1-D)
W dimensionless load parameter
(1-D), $W=w/(E'R)$
(2-D), $W=F/(E'R_x^2)$
x coordinate in direction of flow
X dimensionless coordinate
(1-D), $X=x/b$
(2-D), $X=x/a$
y coordinate
Y dimensionless coordinate, $Y=y/a$
z pressure viscosity parameter (Roelands)

Greek letters

α pressure viscosity index
$\bar{\alpha}$ dimensionless parameter, $\bar{\alpha}=\alpha p_h$
γ constant
ϵ coefficient
η viscosity
η_0 viscosity at ambient pressure
η' lubricant parameter in density–pressure equation
$\bar{\eta}$ dimensionless viscosity, $\bar{\eta}=\eta/\eta_0$
λ dimensionless speed parameter
(1-D), $\lambda=(6\eta_0 u_s R^2)/(b^3 p_h)$
(2-D), $\lambda=(6\eta_0 u_s R_x^2)/(a^3 p_h)$
ν Poisson's ratio
ρ density
ρ_0 density at ambient pressure
$\bar{\rho}$ dimensionless density, $\bar{\rho}=\rho/\rho_0$
$\bar{\rho}^*$ equivalent dimensionless density

Subscripts

x, y x, y direction
m minimum
c central
i grid index
i$=i$ (1-D)
i$=(i, j)$ (2-D)
i grid index (1-D)
i, j grid index (2-D)
approximation
1, 2 contacting body 1, 2
a, b inlet, outlet

Superscripts

i incompressible
c compressible